

Decoupling between first sound and second sound in dilute ^3He – superfluid ^4He mixtures

T. S. Riekkilä,* M. S. Manninen, and J. T. Tuoriniemi
*Low Temperature Laboratory, Department of Applied Physics,
Aalto University, P.O. BOX 15100 FI-00076 AALTO*

(Dated: November 12, 2021)

Bulk superfluid helium supports two sound modes: first sound is an ordinary pressure wave, while second sound is a temperature wave, unique to inviscid superfluid systems. These sound modes do not usually exist independently, but rather variations in pressure are accompanied by variations in temperature, and vice versa. We studied the coupling between first and second sound in dilute ^3He – superfluid ^4He mixtures, between 1.6 K and 2.2 K, at ^3He concentrations ranging from 0 to 11 %, under saturated vapor pressure, using a quartz tuning fork oscillator. Second sound coupled to first sound can create anomalies in the resonance response of the fork, which disappear only at very specific temperatures and concentrations, where two terms governing the coupling cancel each other, and second sound and first sound become decoupled.

PACS numbers: 67.60.-g, 67.25.dt

I. INTRODUCTION

There exist two possible sound modes in bulk superfluid helium: first sound is an ordinary pressure (or density) wave, whereas second sound is a temperature (or entropy) wave. Second sound is unique to superfluid systems, where temperature fluctuations can propagate as waves due to the existence of two independent velocity fields of normal fluid and superfluid component. In normal systems all temperature fluctuations are so strongly damped that such a wave cannot exist. In terms of Tisza's^{1,2} and Landau's³ two-fluid model for superfluid helium, first sound is the mode where normal fluid and superfluid component oscillate in phase, while in second sound they oscillate antiphase. Since ^3He in dilute ^3He – ^4He mixtures is in normal state, it flows with the normal fluid component, which gives another interpretation for second sound: ^3He concentration wave.

First sound and second sound do not usually exist independent from each other, but rather pressure fluctuations of first sound are accompanied by second sound's fluctuations in temperature, and vice versa. In pure ^4He , the coupling is due to the thermal expansion of the liquid, even though it is extremely small. The addition of ^3He modifies, not only the superfluid transition temperature of ^4He , but also the coupling between the two sound modes. In this paper, we show that it is possible to find conditions where second sound and first sound become decoupled from each other, when thermal expansion contribution and ^3He contribution to the coupling cancel each other.

Our studies were conducted using quartz tuning forks, which are commercially mass produced piezoelectric oscillators, whose intended frequency is usually around 32 kHz. They can be used to measure, for example, temperature, pressure, concentration, viscosity, and turbulence in liquid helium⁴⁻⁷. Velocity of second sound in superfluid helium is of order 10 m/s, and its characteristic wavelength, at the used frequency, matches the di-

mensions of common quartz tuning forks. Consequently, at certain temperatures, second sound is able to form standing waves in the fluid surrounding the fork, whereas first sound, with velocity of order 100 m/s, is usually not. When the sound modes are coupled, second sound can drive first sound, and the effect of this driven first sound can be seen as an anomaly in the resonance response of the fork.

These kind of anomalies in the quartz tuning fork response, or second sound resonances, have been observed before⁸⁻¹⁰, but the detailed mechanism producing these anomalies has not been thoroughly investigated. Calculations of the coupling factors between first and second sound in helium mixtures have been presented before by Brusov *et al.*¹¹, but, as first noticed by Rysti¹², they made a sign error in their calculations, which prevented them from noticing the decoupling behavior.

Before presenting the results of our experiment, we first go briefly over the revised calculation of the coupling factors governing the conversion between first sound and second sound.

II. SOUND CONVERSION

Coupling between first sound and second sound in pure ^4He is due to the thermal expansion of the liquid which connects changes in temperature to changes in pressure and vice versa. Since the thermal expansion coefficient of superfluid ^4He is extremely small, the coupling between the sound modes is very weak. The addition of the lighter isotope ^3He modifies the coupling so that at low concentrations the coupling becomes even weaker, eventually vanishing at specific temperatures and concentrations. As the concentration is further increased, the ^3He contribution to the coupling starts to dominate the system and the coupling grows stronger.

We can obtain expressions for sound conversions by starting from the linearized two-fluid hydrodynamical

equations presented by Khalatnikov¹³, from which we reach a set of equations characterizing the sound propagation in ³He-⁴He mixtures

$$\frac{\partial^2 \rho}{\partial t^2} = \nabla^2 P, \quad (1)$$

$$\frac{\rho_n}{\rho_s \sigma} \frac{\partial^2 \sigma}{\partial t^2} = \sigma \nabla^2 T + c \nabla^2 \left(\frac{Z}{\rho} \right), \text{ and} \quad (2)$$

$$\frac{1}{\sigma} \frac{\partial \sigma}{\partial t} = \frac{1}{c} \frac{\partial c}{\partial t}. \quad (3)$$

Here ρ , t , P , σ , T , and c are density, time, pressure, specific entropy, temperature, and ³He mass concentration, respectively, whereas $\rho_n(\rho_s)$ is normal fluid (superfluid) density. Furthermore, $Z \equiv \rho(\mu_3 - \mu_4)$, where μ_3 and μ_4 are the chemical potentials of ³He and ⁴He, respectively. Eq. (1) is the first sound wave equation, Eq. (2) the second sound wave equation, and Eq. (3) is the result of the conservation of entropy and ³He ‘‘impurities’’.

Next, we can choose T , P , and c to be our independent variables, and consider small perturbations around their equilibrium values, so that $T = T_0 + \tilde{T}(\mathbf{r}, t)$, where T_0 is the equilibrium value, and \tilde{T} the small deviation, and similarly for the other variables. We further assume that the perturbations are of plane wave form $\propto \exp(i\omega(\frac{z}{u} - t))$, where ω is the angular frequency, u the velocity of the wave, and z the direction of propagation. When we next eliminate c from eqs. (1)-(3) we obtain a linear set of equations of form

$$A_{00}(u^2)\tilde{T} + A_{01}(u^2)\tilde{P} = 0 \quad (4)$$

$$A_{10}(u^2)\tilde{T} + A_{11}(u^2)\tilde{P} = 0 \quad (5)$$

where Eq. (4) is the linearized first sound wave equation, and Eq. (5) the linearized second sound wave equation. If we assume that the eigenvalues of this system are pure first sound (u_1) and pure second sound (u_2), we can consider the two equations above independently. In order to see how second sound creates first sound, we insert $u = u_2$ in the first sound wave equation (4) *i.e.* we use second sound as source for the first sound. This way, with appropriate simplifications, we get

$$\begin{aligned} \tilde{P} &= -\frac{A_{00}(u_2^2)}{A_{01}(u_2^2)}\tilde{T} \\ &= \left[\left(\frac{\partial \rho}{\partial T} \right)_{P,c} + \frac{c_0}{\bar{\sigma}} \left(\frac{\partial \rho}{\partial c} \right)_{T,P} \left(\frac{\partial \sigma}{\partial T} \right)_{P,c} \right] \frac{u_1^2 u_2^2}{u_1^2 - u_2^2} \tilde{T} \\ &\equiv \alpha \tilde{T}, \end{aligned} \quad (6)$$

where $\bar{\sigma} \equiv \sigma_0 - c_0 \frac{\partial \sigma}{\partial c}$, and α is the coupling factor governing conversion of second sound into first sound. Similarly, if we insert $u = u_1$ in the second sound wave

equation (5), we obtain

$$\begin{aligned} \tilde{T} &= -\frac{A_{11}(u_1^2)}{A_{10}(u_1^2)}\tilde{P} = \frac{U_1^2 \left(\frac{\partial \rho}{\partial T} \right)_{P,c} + c_0 \bar{\sigma} \left(\frac{\partial \rho}{\partial c} \right)_{T,P}}{\rho_0^2 \bar{\sigma}^2 - \rho_0^2 U_1^2 \left(\frac{\partial \sigma}{\partial T} \right)_{P,c}} \tilde{P} \\ &\equiv \beta \tilde{P}, \end{aligned} \quad (7)$$

where $U_1^2 \equiv u_1^2 \frac{\rho_n}{\rho_s} - c_0^2 \left(\frac{\partial(Z/\rho)}{\partial c} \right)_{T,P}$, and β is the coupling factor characterizing conversion of first sound into second sound. These equations are similar to what Brusov *et al.*¹¹ had obtained, except that, as noted by Rysti¹², they made a sign error in the bracketed term of Eq. (6), which prevented them from noticing the possibility of decoupling between the two sound modes. For superfluid helium $(\partial \rho / \partial T)_{P,c}$, which is proportional to the thermal expansion coefficient, is positive, and since $c_0 / \bar{\sigma}$, and $(\partial \sigma / \partial T)_{P,c}$ are also positive, but $(\partial \rho / \partial c)_{T,P}$ is negative, it is possible that the two terms in brackets cancel out each other at certain ³He concentrations and temperatures, resulting in first sound decoupling from second sound. The velocity term of α does not change sign since $u_1 > u_2$ always. On the other hand, the coupling factor β is small, always negative, and practically constant in the temperature and concentration region of our experiment. Only very close to ⁴He superfluid transition temperature, T_λ , its value starts to depart from the constant value. Since β is always finite, first sound can always generate second sound in the region considered here, whereas there exists specific temperatures and concentrations where the opposite is not possible; second sound cannot always create first sound.

Fig. 1 shows the decoupling conditions, as well as calculated values for the bracketed term of the coupling factor α , obtained by using the entropy data of Refs. [14–16], and by evaluating the superfluid and normal fluid densities in mixture according to Refs. [12, 17–20]. Furthermore, the density of the mixture was evaluated by using molar volume formula given by Dobbs²¹, and the pure ⁴He density formula given by Niemela and Donnelly²² scaled by the ³He concentration dependence of T_λ , to produce correct density behavior near T_λ .

At $0.75T_\lambda \approx 1.6$ K, the decoupling occurs already around 0.3% molar ³He concentration, and at higher temperatures the decoupling condition moves to higher concentrations, up to about 3% near T_λ .

III. EXPERIMENTAL DETAILS

Our 2 cm³ experimental cell, shown in Fig. 2, was a simple copper container that had two horizontal tubes soldered at the bottom to house two quartz tuning forks. The copper container itself acted as a buffer volume to ensure that the liquid in the cell was always under saturated vapor pressure, and that the forks were always properly immersed in liquid. The cell was installed in a glass dewar, which could be filled with liquid ⁴He and

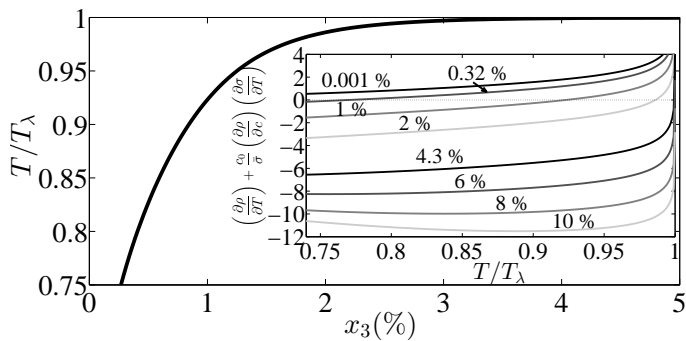


Figure 1: Calculated temperature relative to ${}^4\text{He}$ superfluid transition temperature, $T_\lambda = T_\lambda(x_3)$, where first sound decouples from second sound ($\alpha = 0$), as a function of molar ${}^3\text{He}$ concentration, x_3 . *Inset* shows the values of the bracketed term of α in Eq. (6) as a function of relative temperature at different ${}^3\text{He}$ concentrations.

then pumped to reach temperatures down to about 1.6 K. The temperature of the glass dewar was adjusted by combination of throttling the pumping and a computer controlled heater. Temperature was monitored with two carbon resistors: one was placed directly on the cell, while the other was fixed on the support structure. Cell and bath pressure were measured using *Pfeiffer Vacuum PCR 280* pressure gauges. The carbon resistors were calibrated against the vapor pressure during pure ${}^4\text{He}$ measurements.

${}^3\text{He} - {}^4\text{He}$ mixtures were prepared at room temperature. We started with 25 mmol of commercial quality pure ${}^4\text{He}$ and systematically added mixture of known concentration to obtain the desired composition, finally ending up with 94 mmol of 9% molar concentration mixture. After that, we conducted measurements using mixture taken directly from 6.0%, and 11.0% storage tanks. We used these measurements to calibrate our quartz tuning fork to cross check the concentrations of the earlier used mixtures.

A. Quartz Tuning Fork

We used *ECS-327-8-14X* 32.768 kHz quartz tuning fork oscillator, which was excited by a function generator, and the signal was detected by a lock-in amplifier. We also had another fork with a different resonance frequency and larger physical size installed, but it behaved erratically, and it then could not be used to produce any meaningful experimental data. We measured the fork in so-called tracking mode⁸, in which a computer program determines the resonance frequency and the width of the resonance from a single measurement point close to the actual resonance frequency, assuming that the shape of the resonance is Lorentzian. The tracking mode enables us to repeat the measurement every few seconds instead

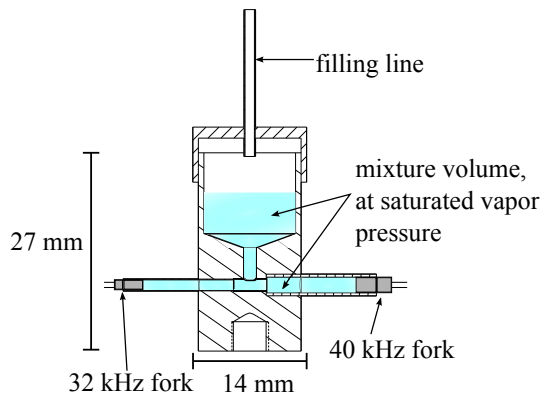


Figure 2: Schematic drawing of the ${}^3\text{He}-{}^4\text{He}$ mixture cell. The buffer volume above the horizontal quartz tuning fork volume helps maintain the liquid under saturated vapor pressure.

of minutes, as it would take if we were to record entire resonance spectra.

Quartz tuning forks do not respond to the temperature of the liquid directly, rather they sense it through the change in viscosity and density of the liquid due to temperature. This means that a standing second sound wave is invisible to the fork, as it cannot cause piezoelectric response.

But second sound can create first sound. Such driven first sound has the same wave characteristics as the second sound wave that is generating it, but as pressure wave, it can push on the fork causing a piezoelectric response. When the first sound decouples from second sound, standing second sound wave is no longer able to drive first sound, and the anomaly in the fork resonance behavior disappears.

These anomalies, caused by first sound driven by second sound, are usually simply called second sound resonances, even if it is slightly inaccurate. The velocity of second sound ranges approximately between 0 m/s and 40 m/s, in the temperature and concentration range of our experiment. Largest values are obtained at low temperatures and at high concentrations, while near T_λ it tends to zero, as second sound ceases to exist^{8,23-26}. Since the second sound velocity has a significant temperature and concentration dependence, there exist numerous possible standing sound wave modes that can be observed with a quartz tuning fork²⁷.

We do not know the exact shape of the standing wave mode within the liquid surrounding the fork. This would be rather difficult to determine as the geometry of the fork is non-trivial. But, the quantity of interest here is the coupling between first sound and second sound, and this is independent from the quartz oscillator. The fork geometry only determines how many second sound resonances we are able to see, at which temperature and concentration they appear, and how strong an anomaly they create.

The wave mode generated by the quartz tuning fork

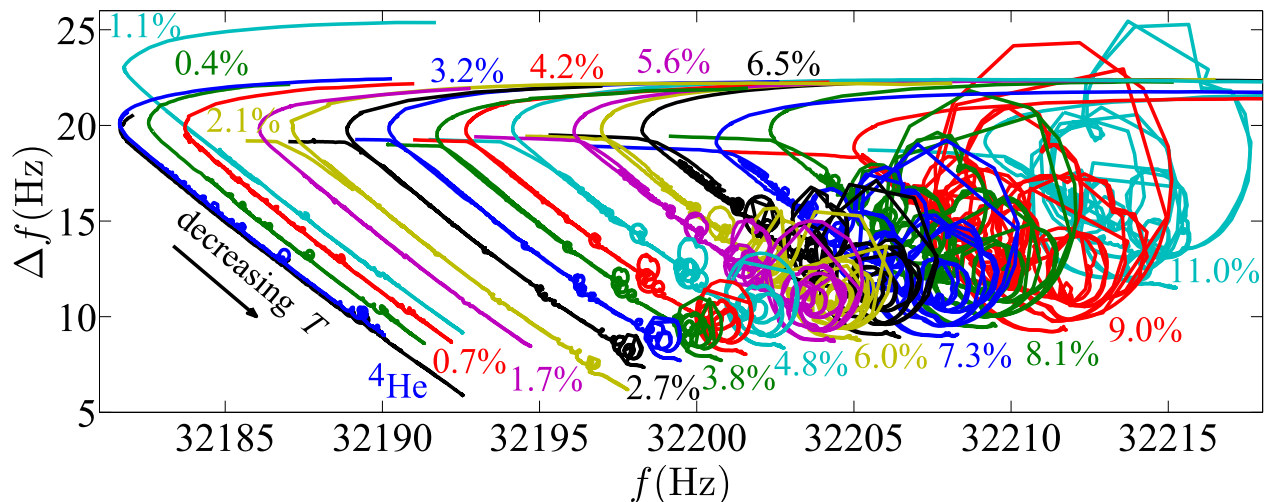


Figure 3: Resonance width (Δf) of the 32 kHz quartz tuning fork versus its resonance frequency (f) with number of ^3He concentrations. The figure contains temperature sweeps both down and up, falling basically on top of each other. The λ -point appears as tilted V-shape near 20 Hz width, and below that the linear decline is due to change in temperature. Second sound resonances appear as loops, whose magnitude is proportional to the coupling strength between second and first sound. There are two pure ^4He measurement sets to demonstrate the reproducibility. Also, note that the 11.0% dataset does not include the lowest temperature resonances as it was done faster than the other sweeps. Its purpose was to be a reference point for our ^3He concentration analysis.

is likely not just pure first sound, but rather some combination of first and second sound. Second sound contribution generated by the fork can couple back through single sound conversion (second sound to first sound), and first sound contribution through double sound conversion (first sound to second sound and back to first). In a single conversion, the coupling factor is just α , but in a double conversion the amplitude of the resonating first sound mode is proportional to the product of the coupling factors, $\alpha\beta$. But since only the coupling factor α has a significant temperature and ^3He concentration dependence, it chiefly determines the coupling/decoupling behavior. The slim temperature dependence of β meant that, we were not able to discern whether the pressure wave affecting the fork had come about through single sound conversion from second sound generated by the fork, or through double sound conversion from first sound generated by the fork. The bottom line is that the determining factor is the coupling coefficient α . When it becomes very small, in either case, second sound can no longer drive first sound, and there would then no longer exist a first sound mode that can couple back to the fork altering its resonance behavior.

IV. RESULTS

Temperature sweeps were carried out from λ -point, down to about 1.6 K and back. Near T_λ the sweep rate had to be quite slow, 0.5 mK/min, since there were many small second sound resonances there. Below about 2 K,

we could increase the rate to 1.5 mK/min as the resonances became more infrequent, and wider in temperature. Fig. 3 shows the resonance frequency of the 32 kHz quartz tuning fork versus resonance width at different ^3He concentrations. In this presentation, anomalies caused by second sound appear as loops. The second sound resonances appeared on same temperature independent of the direction of the temperature sweep, to better than ± 0.6 mK. Pure ^4He was measured multiple times, both before and after the mixture measurements, from which we could estimate the reproducibility to be about ± 3 mK. This spread is due to uncertainty in our temperature determination with the carbon resistors, rather than any variation in the sound properties. Starting from 2.1% ^3He concentration, there appears a horizontal feature near the λ -point, which is caused by the mixing of the helium isotopes. They do not mix properly until near T_λ , after which the fork resonance frequency changes rapidly to a new value.

The 1.1% dataset is shifted with respect to others due to some unknown unreproducible phenomenon, possibly related to some impurities sticking to the fork. We reached this conclusion since the problem did not repeat itself after we had warmed our cooling system back to room temperature between measurements. These data can be made compatible with the others by simple shift, bringing the kink at the λ -point to the appropriate position. We emphasize that Fig. 3 displays the raw data as measured, with no adjustment or post processing.

Since the sound mode coupling in pure ^4He is caused only by the very small thermal expansion, the magnitude of the loops is also quite small. Remarkably, they become

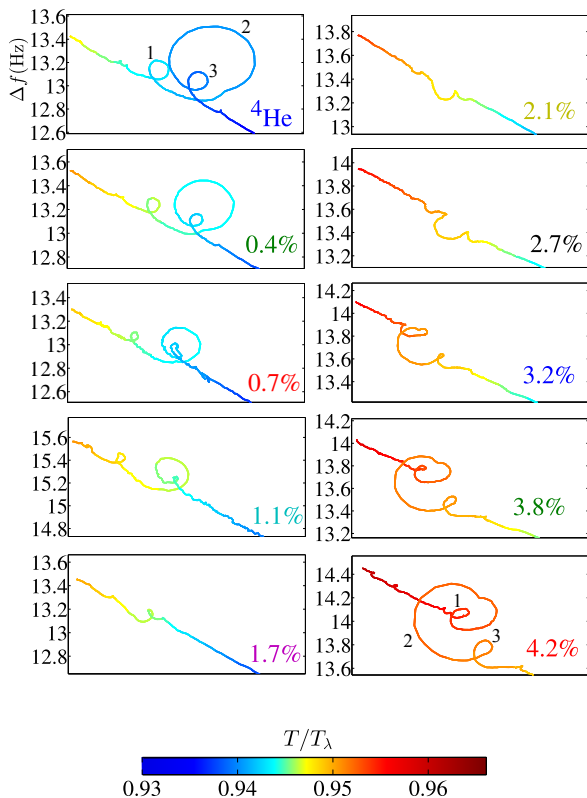


Figure 4: Closer view of the largest high temperature second sound resonances of Fig. 3, followed through the decoupling region. The color of the line changes according to temperature, showing that the resonances move to a higher relative temperature as the ^3He concentration increases. Even though the shape of the resonances changes, we can still identify the three biggest resonances of pure ^4He also in 4.2% mixture.

even smaller as some amount of ^3He is added. The addition of ^3He initially weakens the coupling between the sound modes, as was predicted by our calculations of the coupling factor α in Section II. The second sound anomalies vanish somewhere between 1.1% and 2.1% concentrations, which is indicative of the decoupling between the two sound modes. As the ^3He concentration is further increased, the second sound resonances reappear, eventually becoming significantly larger than they were in pure ^4He , because now the ^3He contribution to the coupling is dominant.

What is more, at 2.1% concentration, there appears a new set of second sound resonances at the low temperature end of the sweep, which were absent in pure ^4He . Temperature sweeps between pure ^4He and 2.1% ^3He concentration, except for 1.1% measurement, were not extended down to the lowest reachable temperature, since we had not initially expected to find anything there. Since the 1.1% sweep continued to a lower temperature than the ones next to it, we can conclude that these resonances had not yet appeared at this concentration.

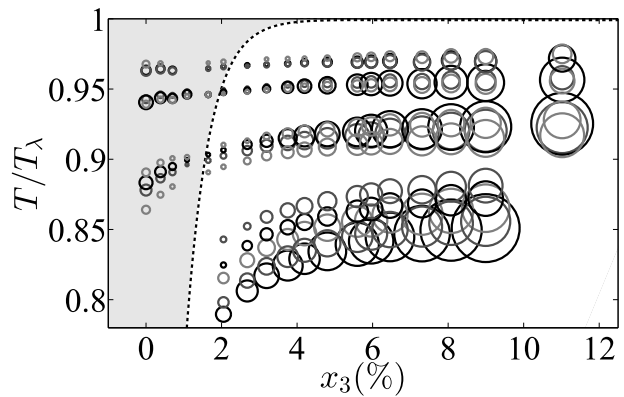


Figure 5: Locations of the second sound resonances followed through the decoupling region in ^3He concentration – relative temperature plane, as well as their amplitude (represented by the size of the circle). Dashed line corresponds the dashed line of Fig. 6, which separates the second sound resonances before the decoupling from those after the decoupling.

^3He concentrations shown in Fig. 3 were obtained by making a linear fit to the background decline of each temperature sweep, and using 6.0%, and 11.0% concentrations as reference points, since their mixture was taken directly from room temperature storage tanks with known concentrations. The uncertainty of all concentrations was estimated to be ± 0.3 percentage points. The concentration values obtained from the tuning fork analysis were roughly 0.5 percentage points less than the concentration estimated while preparing the gas mixture at room temperature.

In Fig. 4, we take a closer look of one set of second sound resonances illustrating their behavior near the decoupling region. Even though their shape changes as the ^3He concentration is increased, we can still identify the correspondent second sound resonances because they always appear in the same sequence — a larger resonance flanked by two smaller resonances, plus a number of tinier ones, in our example. When the coupling is at its weakest, only the large resonance remains barely visible, and it too would seem to disappear somewhere between 1.7% and 2.1% concentrations. Even if the fork resonance width of the 1.1% measurement set is in slightly different range than the others, when also considering temperature, that dataset fits in quite well with the others.

We determined the amplitude for each second sound resonance as the maximum deviation from the fork's background slope, and they were then normalized to the value in the 9.0% measurement set. The temperature of each resonance was defined to be the point of the maximum deviation. These are shown in Fig. 5. Not all second sound resonances of Fig. 3 are included, but rather the selected few that we were able to follow through the decoupling region with sufficient certainty. At high tem-

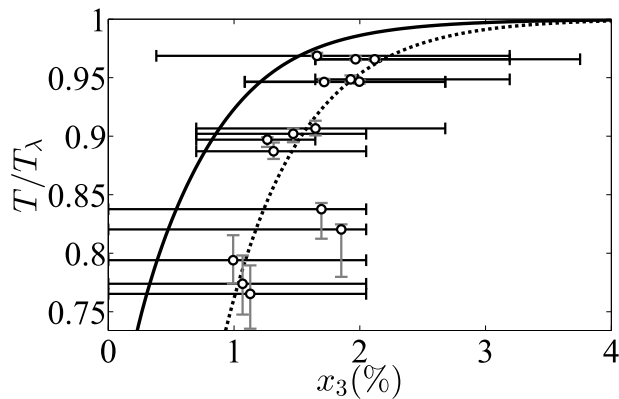


Figure 6: Decoupling temperatures and concentrations interpolated from experimental data compared to the calculated data shown by the solid line (*cf.* Fig. 1). Dashed line is guide to the eye drawn through the evaluated decoupling points.

peratures, or at high concentrations, the anomalies appear almost at the same relative temperature, but otherwise they start to bend to lower temperatures.

The amplitude data allows us to interpolate the locations where the second sound resonances would disappear, as the sound modes become decoupled. These are shown in Fig. 6, where they are compared against the decoupling behavior calculated in Section II. The errorbars were determined from concentrations and temperatures where the anomalies had definitely not yet disappeared, or had definitely appeared again. We also extrapolated the lowest temperature second sound resonance data to find where they would disappear, and since they were not visible in pure ^4He , their errorbars extend all the way to zero concentration. Decoupling points determined from our measurements lie systematically at higher ^3He concentrations than the calculated values. This would suggest that either the ^3He contribution to the coupling is

slightly smaller than the calculations indicated, or that there exists some additional coupling contribution that we had not taken into account.

V. CONCLUSIONS

We studied coupling between first sound and second sound in ^3He – superfluid ^4He mixtures, down to 1.6 K temperature under saturated vapor pressure. Velocity of second sound is such that it can form standing waves around a quartz tuning fork immersed in superfluid. Second sound drives first sound with the same geometry, and this first sound perturbation can be detected by the fork as an anomalous resonance behavior. Since the specific second sound resonances always appear under the same conditions due to the nature of standing waves, they can be used, for example, to indicate fixed points of temperature with good accuracy¹⁰.

We confirmed, that at certain concentrations and temperatures, these second sound anomalies briefly disappear, before reappearing as the ^3He concentration is increased. This behavior is a result of the competing contributions to the coupling between the two sound modes. When the sound modes become decoupled, the standing second sound wave can still exist, but it can no longer create first sound, and hence it becomes invisible to the quartz tuning fork. Our calculations, that revised the results presented in an earlier publication¹¹, predicted exactly this kind of behavior, but they projected the decoupling to occur at somewhat lower ^3He concentration.

ACKNOWLEDGMENTS

We thank J. Rysti for valuable discussions. This work was supported by the Academy of Finland CoE 20122017, Grant No. 250280 LTQ. We also acknowledge the provision of facilities by Aalto University at OtaNano - Low Temperature Laboratory.

* tapio.riekki@aalto.fi

¹ L. Tisza, *Nature* **141**, 913 (1938).

² L. Tisza, *Phys. Rev.* **72**, 838 (1947).

³ L. Landau, *Phys. Rev.* **60**, 356 (1941).

⁴ R. Blaauwgeers, M. Blazkova, M. Clovecko, V. B. Eltsov, R. de Graaf, J. Hosio, M. Krusius, D. Schmoranzner, W. Schoepe, L. Skrbek, P. Skyba, R. E. Solntsev, and D. E. Zmeev, *J. Low Temp. Phys* **146**, 537 (2007).

⁵ A. P. Sebedash, J. T. Tuoriniemi, E. M. M. Pentti, and A. J. Salmela, *J. Low Temp. Phys.* **150**, 181 (2008).

⁶ E. M. Pentti, J. T. Tuoriniemi, A. J. Salmela, and A. P. Sebedash, *Phys. Rev. B* **78**, 1 (2008).

⁷ D. I. Bradley, M. J. Fear, S. N. Fisher, A. M. Guenault, R. P. Haley, C. R. Lawson, P. V. E. McClintock, G. R. Pickett, R. Schanen, V. Tsepelin, and L. A. Wheatland,

J. Low Temp. Phys. **150**, 181 (2008).

⁸ E. M. M. Pentti, J. Rysti, A. J. Salmela, A. P. Sebedash, and J. T. Tuoriniemi, *J. Low Temp. Phys.* **165**, 132 (2011).

⁹ A. J. Salmela, J. T. Tuoriniemi, and J. Rysti, *J. Low Temp. Phys* **162**, 678 (2011).

¹⁰ A. J. Salmela, J. T. Tuoriniemi, E. M. M. Pentti, A. P. Sebedash, and J. Rysti, *JPCS* **150**, 012040 (2009).

¹¹ P. Brusov, J. M. Parpia, P. Brusov, and G. Lawes, *Phys. Rev. B* **63**, 140507(R) (2001).

¹² J. Rysti, *Microscopic and Macroscopic Studies of Liquid and Solid Helium Mixtures*, Ph.D. thesis, Aalto University School of Science, O. V. Lounasmaa Laboratory (2013).

¹³ I. M. Khalatnikov, *An Introduction to the Theory of Superfluidity* (Westview Press, 2000).

¹⁴ T. R. Roberts, R. H. Sherman, S. G. Sydorik, and F. G.

- Brickwedde, Prog. Low Temp. Phys. **4**, 480 (1964).
- ¹⁵ H. C. Kramers, J. D. Wasscher, and C. J. Gorter, Physica **18**, 329 (1952).
- ¹⁶ R. W. Hill and O. V. Lounasmaa, Phil. Mag, **2**, 143 (1957).
- ¹⁷ J. Wilks, *Liquid and Solid Helium* (Clarendon Press, 1967).
- ¹⁸ G. Baym and C. Pethick, The Physics of Liquid and Solid Helium Part II **29**, 123 (1978).
- ¹⁹ M. S. Manninen, *Oscillations on helium surfaces*, Ph.D. thesis, Aalto University School of Science, Department of Applied Physics, Low Temperature Laboratory (2015).
- ²⁰ R. J. Donnelly and C. F. Barengi, J. Phys. Chem. Ref. Data **27**, 1217 (1998).
- ²¹ E. R. Dobbs, *Helium Three* (Oxford University Press, 2000).
- ²² J. J. Niemela and R. J. Donnelly, J. Low Temp. Phys **98**, 1 (1995).
- ²³ C. T. Lane, H. A. Fairbank, and W. M. Fairbank, Phys. Rev. **71**, 600 (1947).
- ²⁴ R. D. Maurer and M. A. Herlin, Phys. Rev. **76**, 948 (1949).
- ²⁵ D. de Klerk, R. P. Hudson, and J. R. Pellam, Phys. Rev. **93**, 28 (1954).
- ²⁶ J. C. King and H. A. Fairbank, Phys. Rev. **93**, 21 (1954).
- ²⁷ J. T. Tuoriniemi, J. Rysti, A. J. Salmela, and M. S. Manninen, JPCS **400**, 1 (2012).